

Synthesis of Palladium Nanoparticles Supported on Mesoporous N-Doped Carbon and Their Catalytic Ability for Biofuel Upgrade

Xuan Xu, Yi Li, Yutong Gong, Pengfei Zhang, Haoran Li, and Yong Wang*

Key Lab of Applied Chemistry of Zhejiang Province, Department of Chemistry, Zhejiang University, Hangzhou 310028, P. R. China

S Supporting Information

ABSTRACT: We report a catalyst made of Pd nanoparticles (NPs) supported on mesoporous N-doped carbon, Pd@CN_{0.132}, which was shown to be highly active in promoting biomass refining. The use of a task-specific ionic liquid (3-methyl-1-butylpyridine dicyanamide) as a precursor and silica NPs as a hard template afforded a high-nitrogen-content (12 wt %) mesoporous carbon material that showed high activity in stabilizing Pd NPs. The resulting Pd@CN_{0.132} catalyst showed very high catalytic activity in hydrodeoxygenation of vanillin (a typical model compound of lignin) at low H₂ pressure under mild conditions in aqueous media. Excellent catalytic results (100% conversion of vanillin and 100% selectivity for 2-methoxy-4-methylphenol) were achieved, and no loss of catalytic activity was observed after six recycles.

Catalysts are the philosopher's stones of the chemical industry. In principle, one can use solids, small organic molecules, or enzymes as catalysts. However, because of the ease of catalyst separation after the reaction, solid catalysts are the preferred options for most processes and dominate the chemical industry (it is estimated that 80–85% of the processes use solid catalysts).¹ Basically, a solid catalyst consists of an active phase (metal or metal oxide) and a high-surface-area porous support on which the active phase is finely dispersed.^{2,3} Notably, the catalytic activity of a solid catalyst can be significantly enhanced by suitably controlling and selecting the support.^{4,5} Characteristics of the support that have been proposed to play a key role in determining the overall reactivity include acid–base properties, redox properties, and the strength of the metal–support interaction.^{4–6}

There are many kinds of materials that are suitable as supports, among which metal oxides (e.g., Al₂O₃,⁷ ZrO₂,⁸ and TiO₂,⁹), zeolites,¹⁰ and carbons (including carbon black, activated carbon, carbon nanofibers, and carbon nanotubes)^{4,5,11,12} are the most frequently used. As carbon materials are mainly composed of carbon and even can be made directly out of biomass, they are obviously the most “sustainable” host materials for metal nanoparticles (NPs). However, noble metals (e.g., Pt, Pd, and Ru) deposited on carbons easily leach during catalytic processes because the interaction between the metal NPs and the carbon surface is weak, and the chemical or catalytic properties of carbons do not always satisfy the sharply increasing demands of catalysis. Therefore, modification of carbons is necessary in most cases.^{5,13} Typically, without

defects, single-walled carbon nanotubes (SWNTs) cannot effectively anchor Pd NPs.¹⁴ In fact, carbons are generally oxidized with H₂O₂ or HNO₃ before use as host materials to introduce more defects and strengthen the interaction between the metal NPs and the support.¹⁵

Nitrogen-containing carbons, as a kind of fascinating materials, have attracted worldwide attention recently.^{16,17} They promise access to a wide range of applications because the incorporation of nitrogen atoms in the carbon architecture can enhance chemical, electrical, and functional properties.^{18,19} Among the methods used to prepare N-doped carbon, in situ doping by using nitrogen-containing precursors can realize a homogeneous incorporation of nitrogen into carbons with controlled chemistry.^{20,21} Typical examples include the use of task-specific ionic liquids (ILs) as excellent precursors to produce functional N-doped carbons with controlled pore architectures.^{17,22–25} In this work, focusing on supported Pd NPs as the catalytic agent, we synthesized a kind of N-doped mesoporous carbon (CN_x) by using a nitrogen-containing IL as a suitable precursor and explored its use as a basic host to construct binary Pd@CN_x heterojunctions for biofuel upgrade.

The dicyanamide-containing IL 3-methyl-1-butylpyridine dicyanamide (3-MBP-dca) [Scheme S1 in the Supporting Information (SI)] was chosen as the precursor, envisioning that the cross-linkable anion might result in C–N condensation. An N-doped carbon with both narrowly distributed mesoporosity (Figure 1A) and local N–C–N structural motifs was obtained from the precursor mixture of 3-MBP-dca and 12 nm SiO₂ NPs after condensation at 900 °C for 1 h (Figure S3 in the SI) and removal of SiO₂ template. The as-made N-doped carbon was then used as a support for the loading of Pd NPs by an ultrasound-assisted method.

Elemental analysis indicated that the resulting mesoporous N-doped carbon (denoted as CN_{0.132}) had a N/C atom ratio of 0.132 (Table S2 in the SI). X-ray diffraction (XRD) revealed a graphitic stacking peak at 26.0°, and the more pronounced peak at 43.5° points to the formation of intralayer condensation for the material (Figure 1B). The formation of graphitic order was further proved by the Raman spectrum (Figure 1C), in which the G band at ~1590 cm⁻¹ indicates the in-plane vibration of sp² carbon atoms, while the D band at ~1350 cm⁻¹ is a defect-induced Raman feature representing the nonperfect crystalline structure of the material. The D band appears to be stronger than the G band, indicating the amorphization of the graphitic network because of much higher nitrogen percentage in the

Received: August 16, 2012

Published: October 3, 2012

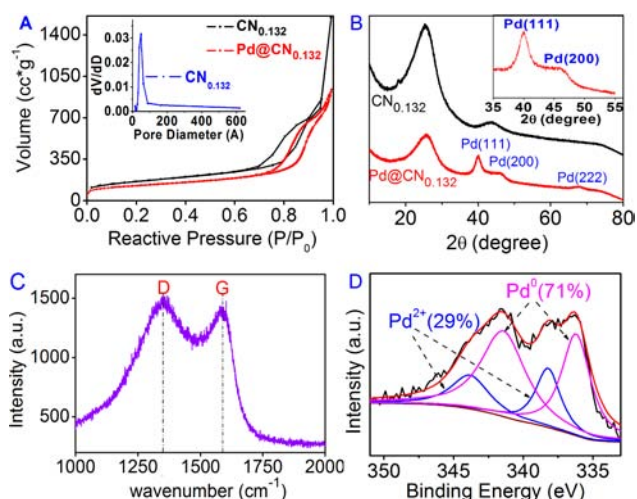


Figure 1. (A) Adsorption/desorption isotherms of $\text{CN}_{0.132}$ (black) and $\text{Pd@CN}_{0.132}$ (red). The inset shows the pore size distribution of $\text{CN}_{0.132}$. (B) XRD patterns of $\text{CN}_{0.132}$ (black) and $\text{Pd@CN}_{0.132}$ (red). (C) Raman spectrum of $\text{CN}_{0.132}$. (D) XPS curve of $\text{Pd@CN}_{0.132}$.

resulting mesoporous carbon. Additional evidence of N doping was provided by X-ray photoelectron spectroscopy (XPS). Figure S4 shows two N 1s peaks corresponding to different binding energies, revealing that in this case, nitrogen is embedded into the graphitic structure mainly in two forms. The N 1s peaks at 398.8 and 401.0 eV are attributed to pyridinic and quaternary nitrogen in the carbon texture, respectively.

$\text{CN}_{0.132}$ has a large nitrogen percentage of 12%; nitrogen in carbon texture is suitable for stabilizing highly dispersed Pd NPs and preventing the reoxidation of Pd^0 . As expected, $\text{Pd@CN}_{0.132}$ contained 71% Pd^0 as revealed by Pd 3d_{5/2} XPS peaks at 336.2 and 341.4 eV (Figure 1, D). The formation of highly dispersed Pd NPs was proven by XRD (Figure 1B) and high-resolution transmission electron microscopy (HRTEM) (Figure 2). The diffraction peaks at 40.0 and 46.6° in the XRD pattern show the characteristic (111) and (200) planes of Pd NPs, respectively. From the (111) diffraction peak and Scherrer's formula, the average size of the crystallites was calculated to be 4.9 nm, in good agreement with the value predicted by HRTEM (4.1 nm). The HRTEM images revealed

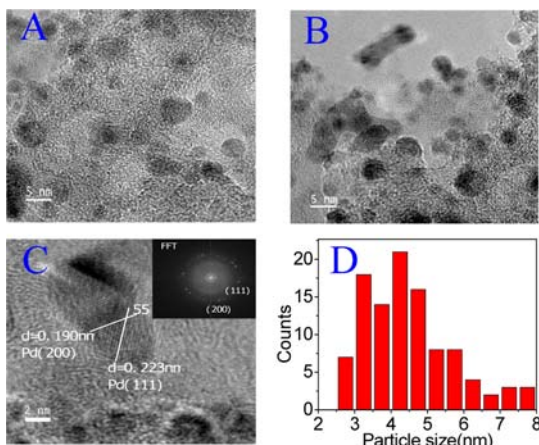


Figure 2. HRTEM images and particle size distribution of $\text{Pd@CN}_{0.132}$.

well-dispersed Pd NPs on the surface of $\text{CN}_{0.132}$. Figure 2C shows two kinds of crystal planes of Pd, and the crystal plane spacings were measured as 0.223 and 0.190 nm, corresponding to the (111) and (200) planes, with a plane angle of 55°.

To illustrate the usefulness of this nanohybrid catalyst, the activity of $\text{Pd@CN}_{0.132}$ for biofuel upgrade was investigated. In the past decades, interest in the production of fuels or commodity chemicals from renewable biomass instead of fossil resources has continued to grow.^{26,27} Compared with cellulose and hemicellulose, lignin, which constitutes ~30 wt % of woody biomass, is challenging to convert, partly because of its highly complex structure, which consists of subunits derived from phenol, *p*-coumaryl, coniferyl, and sinapyl alcohols typically connected with ether linkages.^{28,29} Accordingly, it is more challenging to deoxygenate lignin-derived pyrolysis oil than cellulose-derived pyrolysis oil.^{1,2,30–32} Here we used vanillin (4-hydroxy-3-methoxybenzaldehyde), a common component of pyrolysis oil derived from the lignin fraction, as a substrate to explore the principal hydrogenation and deoxygenation routes (Scheme S2).

Transformation of the carbonyl group into a methyl group theoretically can proceed in three ways: (i) hydrogenation/dehydration, (ii) hydrogenation/hydrogenolysis, and (iii) direct hydrogenolysis of the C=O bond.³³ In our case, there is no H atom at the position adjacent to the hydroxyl group in vanillin alcohol, so dehydration could not happen. Therefore, the transformation of vanillin into 2-methoxy-4-methylphenol must proceed via path (ii) and/or (iii). Figure 3 shows the evolution

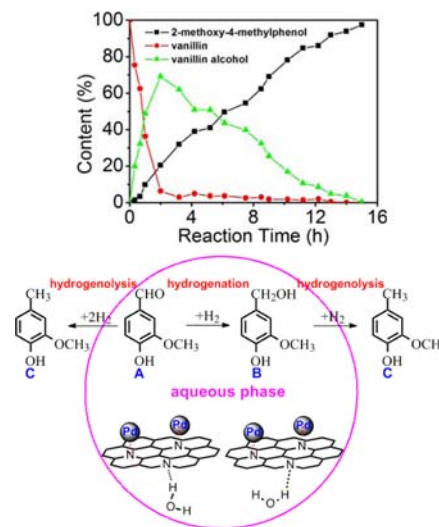


Figure 3. (top) Evolution of reactant and product concentrations with reaction time and (bottom) possible reaction pathway.

of the reactant and product concentrations with reaction time in the experiment performed with vanillin over $\text{Pd@CN}_{0.132}$ at 90 °C under 1 bar H_2 in water. The reaction was accompanied by a rapid increase in vanillin alcohol and a decrease in vanillin in the first 2 h, illustrating that vanillin is mainly hydrogenated to vanillin alcohol in the first step. However, even in the first 20 min, 2-methoxy-4-methylphenol was observed, suggesting that hydrogenolysis of vanillin alcohol occurred or that vanillin underwent via direct hydrogenolysis of C=O as well. Later, hydrogenolysis of vanillin alcohol proceeded rapidly. After 15 h, almost all of the vanillin alcohol had been converted to 2-methoxy-4-methylphenol via hydrogenolysis.

Most recently, Resasco and co-workers achieved both good conversion and selectivity in the hydrodeoxygenation of vanillin by depositing palladium onto SWNT–inorganic oxide hybrid NPs (Pd@SWNT-SiO₂) in a water/oil emulsion. For example, when Pd@SWNT-SiO₂ was used as a catalyst in a biphasic system, 85% of vanillin was consumed in 0.5 h with 47% selectivity for 2-methoxy-4-methylphenol (Table 1, entry 1).

Table 1. Catalytic Results for Different Catalysts

entry	catalyst	solvent	conv. (%)	selectivity (%) ^a	
				B	C
1 ^b	Pd@SWNT-SiO ₂	water and decalin	85	53	47
2 ^c	Pd@CN _{0.132}	water and decalin	100	–	93
3	Pd@CN _{0.132}	water	100	–	100
4	Pd@C	water	98	26	74
5	Pd@TiO ₂	water	98	79	21
6 ^d	Pd@MgO	water	28	32	–
7	Pd@CeO ₂	water	88	86	14
8	Pd@γ-Al ₂ O ₃	water	95	31	69
9 ^e	Pd@CN _{0.132}	water	98	–	100

^aB is the hydrogenation product, 4-hydroxymethyl-2-methoxyphenol, and C is the hydrogenation/hydrogenolysis (or direct hydrogenolysis) product, 2-methoxy-4-methylphenol (see Figure 3). ^b1:1 (v/v) water/decalin; data taken from ref 14. ^c1:1 (v/v) water/decalin. ^dOther byproducts were unidentified. ^eS/C = 1000, H₂ pressure 1.0 MPa, 150 °C, 6 h.

For comparison, we tested the activity of Pd@CN_{0.132} under the same conditions and found that Pd@CN_{0.132} showed remarkably high catalytic activity, giving 100% conversion of vanillin and 93% selectivity for 2-methoxy-4-methylphenol (entry 2). Water is a desirable solvent for chemical reactions for reasons of cost, safety, and environmental impact. We subsequently conducted the reaction in water and found that even better selective hydrodeoxygenation could be achieved, as a 100% yield of 2-methoxy-4-methylphenol was obtained in 0.5 h (entry 3). Moreover, the Pd@CN_{0.132} catalyst was compared with commercially available Pd@C under the same conditions as well as with other oxide-supported Pd NPs, including Pd@TiO₂, Pd@MgO, Pd@CeO₂, and Pd@γ-Al₂O₃. The textural properties of the catalyst supports are shown in Table S4. The results in Table 1, entries 3 and 4 clearly show that the catalyst synthesized here gives better activity and 2-methoxy-4-methylphenol selectivity than commercially prepared Pd@C. Oxide-supported Pd NPs were moderately effective for this reaction, affording 2-methoxy-4-methylphenol in lower yields than Pd@CN_{0.132}. From these results, to a first approximation one could conclude that the nature of the support plays an important role in the activity and selectivity of Pd catalysts for the hydrodeoxygenation of vanillin. We deduced that the hydrophilic property of Pd@CN_{0.132} affects its catalytic performance greatly. It was found that after the reaction, the Pd@CN_{0.132} catalyst dispersed well in water (Figure S5). Compared with the highly aggregated state of the traditional solid catalysts, doping with N atoms increased the hydrophilic property of Pd@CN_{0.132}, which might enhance the catalyst dispersion in water and improve the exposure of the catalyst to the substrates (e.g., vanillin), thereby increasing the catalytic performance significantly.

For practical applications, both high yield and low cost are required. We thus conducted the reaction with an increased

vanillin/Pd (substrate/catalyst) molar ratio of S/C = 350. As demonstrated in Figure 4, a vanillin conversion of 65% with a 2-

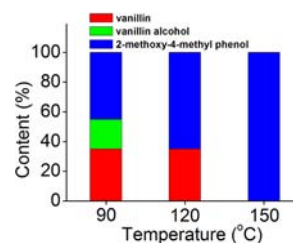


Figure 4. Product distribution at different temperatures. Reaction conditions: vanillin, 1000 mg; S/C = 350; water, 80 mL; H₂ pressure, 1.0 MPa, reaction time, 1 h.

methoxy-4-methylphenol selectivity of 69% was achieved within 1 h at 90 °C. The reaction was accelerated at higher temperature; for example, full conversion with a high 2-methoxy-4-methylphenol selectivity of >99% was obtained in 1 h at 150 °C. For comparison, when Pd@SWNT-SiO₂ was used as the catalyst with a water/oil emulsion as the solvent, a high 2-methoxy-4-methylphenol yield (~95%) was obtained only at a higher temperature of 200 °C with S/C = 100.¹⁴ Notably, we found that 2-methoxy-4-methylphenol is very stable in our reaction systems, as a further increase in temperature to 200 °C did not produce a deeper hydrogenolysis product. We attribute the high 2-methoxy-4-methylphenol yield to its poor solubility in water: when it is formed under the reaction conditions, it separates from the water phase and avoids the further hydrogenolysis to give 2-methoxyphenol. An S/C ratio of 1000 was then tested for the Pd@CN_{0.132} catalyst, and even with this high substrate concentration, the reaction went smoothly and gave 98% conversion of vanillin with 100% selectivity for 2-methoxy-4-methylphenol (Table 1, entry 9).

Furthermore, the catalyst can easily be separated from the reaction solution by simple filtration. The catalyst is highly stable and can be reused for several cycles without losing its activity, which is a prerequisite for practical applications (Table S3). The concentration of Pd in the reaction solution was determined by ICP-AES to be <0.1 ppm, meaning that leaching of Pd into the solvent is negligible. Since nitrogen is strongly electronegative and usually has a lone pair of electrons, the nitrogen functionalities on the surface might act as Lewis base sites and are expected to be more effective in retaining metal NPs.

In conclusion, Pd NPs have been heterogeneously supported on mesoporous N-doped carbon with its special base properties and electronic behavior. The novel Pd catalyst exhibits a high activity for the hydrodeoxygenation of vanillin, a common component in lignin-derived bio-oil, under mild reaction conditions with water as a clean solvent. The high catalytic performance has been attributed to the special structure of the catalytic N-doped carbon–metal heterojunction, which leads not only to a very stable and uniform dispersion of Pd NPs but also to additional electronic activation of the metal NPs and good dispersion of the catalyst in water. This Pd@CN_{0.132} catalyst holds promising potential for the biofuel upgrade process, and further work will be directed toward the applications to natural lignin and other model systems.

■ ASSOCIATED CONTENT**■ Supporting Information**

Experimental and characterization details, Schemes S1 and S2, Figures S1–S6, and Tables S1–S4. This material is available free of charge via the Internet at <http://pubs.acs.org>.

■ AUTHOR INFORMATION**Corresponding Author**

chemwy@zju.edu.cn

Notes

The authors declare no competing financial interest.

■ ACKNOWLEDGMENTS

Financial support from the Joint Petroleum and Petrochemical Funds of the National Natural Science Foundation of China and China National Petroleum Corporation (U1162124), the Fundamental Research Funds for the Central Universities, the Program for Zhejiang Leading Team of S&T Innovation (2011RS0007), and the Partner Group Program of Zhejiang University and the Max Planck Society are greatly appreciated.

■ REFERENCES

- (1) Rinaldi, R.; Schüth, F. *Energy Environ. Sci.* **2009**, *2*, 610.
- (2) Beaumont, S. K. *J. Chem. Technol. Biotechnol.* **2012**, *87*, 595.
- (3) Thomas, J. M.; Johnson, B. F. G.; Raja, R.; Sankar, G.; Midgley, P. A. *Acc. Chem. Res.* **2003**, *36*, 20.
- (4) Wang, Y.; Yao, J.; Li, H.; Su, D.; Antonietti, M. *J. Am. Chem. Soc.* **2011**, *133*, 2362.
- (5) White, R. J.; Luque, R.; Budarin, V. L.; Clark, J. H.; Macquarrie, D. J. *Chem. Soc. Rev.* **2009**, *38*, 481.
- (6) Martono, E.; Vohs, J. M. *J. Catal.* **2012**, *291*, 79.
- (7) Bond, J. Q.; Alonso, D. M.; Wang, D.; West, R. M.; Dumesic, J. A. *Science* **2010**, *327*, 1110.
- (8) Peng, B. X.; Yuan, X. G.; Zhao, C.; Lercher, J. A. *J. Am. Chem. Soc.* **2012**, *134*, 9400.
- (9) Enache, D. I.; Edwards, J. K.; Landon, P.; Solsona-Espriu, B.; Carley, A. F.; Herzing, A. A.; Watanabe, M.; Kiely, C. J.; Knight, D. W.; Hutchings, G. J. *Science* **2006**, *311*, 362.
- (10) Zhang, C.; Lercher, J. A. *Angew. Chem., Int. Ed.* **2012**, *51*, 5935.
- (11) Deng, W. P.; Liu, M.; Tan, X. S.; Zhang, Q. H.; Wang, Y. J. *Catal.* **2010**, *271*, 22.
- (12) Zhao, C.; Kou, Y.; Lemonidou, A. A.; Li, X. B.; Lercher, J. A. *Angew. Chem., Int. Ed.* **2009**, *48*, 3987.
- (13) Clippel, F.; Dusselier, M.; Van Rompaey, R.; Vanelderen, P.; Dijkmans, J.; Makshina, E.; Giebeler, L.; Oswald, S.; Baron, G. V.; Denayer, J. F. M.; Pescarmona, P. P.; Jacobs, P. A.; Sels, B. F. *J. Am. Chem. Soc.* **2012**, *134*, 10089.
- (14) Crossley, S.; Faria, J.; Shen, M.; Resasco, D. E. *Science* **2010**, *327*, 68.
- (15) Radkevich, V. Z.; Senko, T. L.; Wilson, K.; Grishenko, L. M.; Zaderko, A. N.; Diyuk, V. Y. *Appl. Catal., A* **2008**, *335*, 241.
- (16) Yang, S. B.; Feng, X. L.; Wang, X. C.; Müllen, K. *Angew. Chem., Int. Ed.* **2011**, *50*, 5339.
- (17) Lee, J. S.; Wang, X. Q.; Luo, H. M.; Baker, G. A.; Dai, S. *J. Am. Chem. Soc.* **2009**, *131*, 4596.
- (18) Yang, W.; Fellingner, T. P.; Antonietti, M. *J. Am. Chem. Soc.* **2011**, *133*, 206.
- (19) Fulvio, P. F.; Lee, J. S.; Mayes, R. T.; Wang, X. Q.; Mahurin, S. M.; Dai, S. *Phys. Chem. Chem. Phys.* **2011**, *13*, 13486.
- (20) Liu, R.; Mahurin, S. M.; Li, C.; Unocic, R. R.; Idrobo, J. C.; Gao, H. J.; Pennycook, S. J.; Dai, S. *Angew. Chem., Int. Ed.* **2011**, *50*, 6799.
- (21) Zhao, L.; Fan, L. Z.; Zhou, M. Q.; Guan, H.; Qiao, S. Y.; Antonietti, M.; Titirici, M. *Adv. Mater.* **2010**, *22*, 5202.
- (22) Paraknowitsch, J. P.; Zhang, J.; Su, D. S.; Thomas, A.; Antonietti, M. *Adv. Mater.* **2010**, *22*, 87.
- (23) Wang, X. Q.; Dai, S. *Angew. Chem., Int. Ed.* **2010**, *49*, 6664.
- (24) Lee, J. S.; Wang, X. Q.; Luo, H. M.; Dai, S. *Adv. Mater.* **2010**, *22*, 1004.
- (25) Yuan, J. Y.; Giordano, C.; Antonietti, M. *Chem. Mater.* **2010**, *22*, 5003.
- (26) Vispute, T. P.; Zhang, H. Y.; Sanna, A.; Xiao, R.; Huber, G. W. *Science* **2010**, *330*, 1222.
- (27) Huber, G. W.; Iborra, S.; Corma, A. *Chem. Rev.* **2006**, *106*, 4044.
- (28) Zakzeski, J.; Bruijninx, P. C. A.; Jongerius, A. L.; Weckhuysen, B. M. *Chem. Rev.* **2010**, *110*, 3552.
- (29) Mohan, D.; Pittman, C. U., Jr.; Steele, P. H. *Energy Fuels* **2006**, *20*, 848.
- (30) Nimmanwudipong, T.; Runnebaum, R. C.; Block, D. E.; Gates, B. C. *Energy Fuels* **2011**, *25*, 3417.
- (31) Nimmanwudipong, T.; Runnebaum, R. C.; Ebeler, S. E.; Block, D. E.; Gates, B. C. *Catal. Lett.* **2012**, *142*, 151.
- (32) Yan, N.; Yuan, Y.; Dykeman, R.; Kou, Y.; Dyson, P. J. *Angew. Chem., Int. Ed.* **2010**, *49*, 5549.
- (33) Prochazkova, D.; Zamostny, P.; Bejblova, M.; Cervený, L.; Cejka, J. *Appl. Catal., A* **2007**, *332*, 56.